REPORT DOCUMENTATION PAGE

1. REPORT DATE *(DD-MM-YYYY)* 20-07-2012	2. REPORT TYPE Conference Paper	3. DATES COVERED *(From - To)*

4. TITLE AND SUBTITLE

A Comparison of Ion Acceleration Characteristics for Krypton and Xenon Propellants within a 600 Watt hall Thruster

5a. CONTRACT NUMBER

5b. GRANT NUMBER

5c. PROGRAM ELEMENT NUMBER

6. AUTHOR(S)

Hargus Jr., W.A.; Azarnia, G.M.; Nakles, M.R.

5d. PROJECT NUMBER

5f. WORK UNIT NUMBER
33SP0706

7. PERFORMING ORGANIZATION NAME(S) AND ADDRESS(ES)

Air Force Research Laboratory (AFMC)
AFRL/RQRS
1 Ara Drive
Edwards AFB CA 93524-7013

8. PERFORMING ORGANIZATION REPORT NUMBER

9. SPONSORING / MONITORING AGENCY NAME(S) AND ADDRESS(ES)

Air Force Research Laboratory (AFMC)
AFRL/RQR
5 Pollux Drive
Edwards AFB CA 93524-7048

10. SPONSOR/MONITOR'S ACRONYM(S)

11. SPONSOR/MONITOR'S NUMBER(S)
AFRL-RQ-ED-TP-2012-233

12. DISTRIBUTION / AVAILABILITY STATEMENT

Approved for public release; distribution unlimited (PA #12606).

13. SUPPLEMENTARY NOTES

For presentation at the 48th AIAA/ASME/SAE/ASEE Joint Propulsion Conference & Exhibit and 10th International Energy Conversion Engineering Conference, Atlanta, GA, 29 July – 2 August 2012.

14. ABSTRACT

There is growing interest within the electrostatic propulsion community in the use of krypton as a propellant. It is a lower cost replacement for xenon, and is especially of interest for potentially very large solar electric transfer vehicles that may potentially strain xenon production capability. This work compares the internal propellant acceleration of krypton within a laboratory medium power Hall effect thruster to historical xenon data for the same thruster. One case matched in propellant particle flux (matched volumetric flow rates) is presented. The measurements consist of laser-induced fluorescence velocimetry extending approximately the anode to 10 mm outside the thruster into plume along the center of the coaxial acceleration channel. The results show that the acceleration process for krypton is more gradual and produces a lower electric field. As a result, energy conversion is lower than xenon for this flow matched case. In addition, there is clear evidence of ionization throughout the acceleration channel. This may explain a lower performance for krypton as this particular appears to have low propellant utilization. It is not known to what extent the less oscillatory plasma and/or the lower ionization cross-section of the krypton discharge produced this difference relative to xenon.

15. SUBJECT TERMS

16. SECURITY CLASSIFICATION OF:			17. LIMITATION OF ABSTRACT	18. NUMBER OF PAGES	19a. NAME OF RESPONSIBLE PERSON W.A. Hargus Jr.
a. REPORT Unclassified	b. ABSTRACT Unclassified	c. THIS PAGE Unclassified	SAR	10	19b. TELEPHONE NUMBER *(include area code)* N/A

A Comparison of Ion Acceleration Characteristics for Krypton and Xenon Propellants within a 600 Watt Hall Effect Thruster

William A. Hargus, Jr.*
Gregory M. Azarnia†
Michael R. Nakles‡

Air Force Research Laboratory, Edwards Air Force Base, CA 93524

There is growing interest within the electrostatic propulsion community in the use of krypton as a propellant. It is a lower cost replacement for xenon, and is especially of interest for potentially very large solar electric transfer vehicles that may potentially strain xenon production capability. This work compares the internal propellant acceleration of krypton within a laboratory medium power Hall effect thruster to historical xenon data for the same thruster. One case matched in propellant particle flux (matched volumetric flow rates) is presented. The measurements consist of laser-induced fluorescence velocimetry extending approximately the anode to 10 mm outside the thruster into plume along the center of the coaxial acceleration channel. The results show that the acceleration process for krypton is more gradual and produces a lower electric field. As a result, energy conversion is lower than xenon for this flow matched case. In addition, there is clear evidence of ionization throughout the acceleration channel. This may explain a lower performance for krypton as this particular appears to have low propellant utilization. It is not known to what extent the less oscillatory plasma and/or the lower ionization cross-section of the krypton discharge produced this difference relative to xenon.

Introduction

A T present, xenon (Xe) is the propellant of choice for most electrostatic plasma thrusters including Hall effect thrusters. The selection of xenon is due to a number of rigorous engineering rationale. These include the high mass (131 amu) and relatively low ionization potential (12.1 eV) of xenon; as well as the inert nature of xenon, which eliminates much of the controversy that plagued early electrostatic propulsion efforts when mercury (Hg) and cesium (Cs) were the propellants of choice.[1] Although xenon is a noble gas, it is the heaviest, and due to its non-ideal gas behavior, it is possible to pressurize and store with room temperature specific densities approaching 1.6.[2,3] As such, it may be stored at higher densities than that of the most common liquid monopropellant, hydrazine, which as a specific gravity of approximately 1.

While xenon may remain an ideal propellant for electrostatic thrusters such as Hall effect thrusters, there are several concerns that have driven the Hall effect thruster community to explore alternative propellants. As orbit raising missions of longer duration and larger payloads are proposed, requisite propellant mass increases dramatically. Xenon production is a byproduct of the fractional distillation of atmospheric gases for use primarily by the steel industry. Due to the low concentration of xenon in the atmosphere (∼90 ppb), worldwide production is only approximately 6,000 standard cubic meters per year. Increasing industrial demand for items such as high efficiency lighting and windows, as well as plasma based micro-fabrication, has produced wide price swings in the past decade. Xenon prices have varied by as much as factor of ten in the past four years alone.

For missions that can benefit from higher specific impulse, krypton may have benefits beyond its lower cost. Krypton has a lower atomic mass (83.8 amu), but a slightly higher ionization potential (14.0 eV) than xenon. Like xenon, krypton is a noble gas and could be easily integrated into existing Hall effect thruster propellant management systems without significant modification. The similar ionization potential should not dramatically affect Hall effect thruster efficiency, and the lower atomic mass could produce a 25% increase in specific impulse. The increase in specific impulse may be useful for missions such as station-keeping where increased specific impulse is advantageous. For missions such as orbit raising, increasing the specific impulse may increase trip time due to power limitations. However as solar electric

---

*Senior Engineer, AFRL/RZSS, Edwards AFB, CA, USA.
†Engineer, ERC, Inc, Edwards AFB, CA, USA.
‡Engineering Physicist, ERC, Inc., Edwards AFB, CA, USA.

power system specific power decreases, increasing the specific impulse of the propulsion system can maintain trip time while reducing total system mass. Krypton is approximately $10\times$ more common in the atmosphere (and hence in production) than xenon, and when accounting for mass is approximately $6\times$ less expensive. Table 1 summarizes the properties of xenon and krypton.[2]

Table 1   Comparison of xenon and krypton properties critical for electrostatic propulsion.[2]

Property	Units	Xe	Kr
Atomic Mass	amu	131.3	83.8
1st Ionization Energy	eV	12.1	14.0
2nd Ionization Energy	eV	21	24
3rd Ionization Energy	eV	32	37
Atmospheric Concentration	ppb	87	1000
Stable Isotopes		9	6
Odd Isotopes		2	1
Critical Pressure	MPa	5.84	5.50
Critical Temperature	K	290	209
Boiling Point (1 atm)	K	161	120

In order to assess whether the potential advantages of krypton propellant can be realized in Hall effect thrusters and other electrostatic thruster types, experimental measurements of these plasmas must be obtained; both to determine relative figures of functional merit and for numerical simulation validation for increased fundamental understanding of subtle propellant effects. This efforts goal is to begin the comparison of krypton and xenon acceleration in the same thruster under comparable conditions. For one case of matched propellant particle flux (atoms/second), this work compares the internal propellant acceleration of krypton within a laboratory medium power Hall effect thruster to historical xenon data for the same thruster. The comparison has value for both understanding the impacts of subtle changes in propellant as well as for modeling of these thrusters and understanding how those subtle changes can have visible impacts.

Laser-Induced Fluorescence

Laser-induced fluorescence (LIF) may be used to detect velocity–induced shifts in the spectral absorption of various plasma species. The fluorescence is monitored as a continuous-wave laser is tuned in frequency over the transition of interest, of energy $h\nu_{12}$; where h is Plank's constant, ν_{12} is wavenumber of transition between lower state 1 and higher energy state 2. Note that state 1 may be the ground state, but any sufficiently highly populated excited state will do. For the highly excited, but low density accelerated plasmas of interest, we generally choose to examine a metastable state to ensure highest signal levels at convenient excitation wavelengths. Measurements can be made with high spatial resolution as determined by the intersection of probe laser beam with fluorescence optical collection.

Velocity measurements are made using LIF velocimetry as an ion population moving with a velocity component u relative to the direction of the incoming laser absorbs photons at a frequency shifted from that of stationary absorbers due to the Doppler effect. The magnitude of this frequency shift $\delta\nu_{12}$ is

$$\delta\nu_{12} = \frac{u}{c}\nu_{12}. \tag{1}$$

The measured fluorescence lineshape is determined by the environment of the absorbing ion population, so an accurate measurement of the lineshape function may lead to the determination of a number of plasma parameters beyond simple bulk velocities. The precision of measured velocities has been found, in various studies, to be less than the experimental uncertainty for the ions (±500 m/s).[4,5,6] Several factors affect the lineshape and give rise to broadening and/or a shift of the spectral line. In high-temperature plasmas, the most significant is Doppler broadening due to the absorber's random thermal motion, characterized by the atomic, or ionic, kinetic temperature, T_{kin}. When the absorbing species velocity distribution is Maxwellian in shape, the Doppler broadening results in a Gaussian lineshape. Collisional interactions between the absorbers and other species in the plasma give rise to spectral lineshapes that are often Lorentzian. This includes interactions with charged particles (Stark broadening) and uncharged particles (van der Waals broadening). If both Doppler broadening and collisional broadening are important and independent, the resulting lineshape is a convolution of the Gaussian and Lorentzian lineshape into a Voigt lineshape.[7]

LIF is a convenient diagnostic for the investigation of ion velocities in a plasma thruster as it does not physically perturb the discharge. The LIF signal is a convolution of the velocity distribution function (VDF), transition lineshape, and laser beam frequency profile. Determination of the VDF from LIF data only requires the deconvolution of the transition lineshape and laser beam profile from the raw LIF signal trace. Alternatively, the lineshape itself may also provide valuable information on the state of the plasma, such as electron density, pressure, or heavy species temperature. In the somewhat turbulent plasmas typical of Hall effect thrusters, the fluorescence lineshape can also be indicative of the relative motion of the ionization zone as it axially traverses in the periodic breathing mode plasma fluctuation.[8,9] However, care must be taken to ensure that the relative effects of these phenomena are separable. In addition, magnetic (Zeeman effect) and electric (Stark effect) fields may

Table 2 *Nominal thruster operating conditions.*

Kr Anode Flow	25.5 sccm
	(1.59 mg/s)
Kr Cathode Flow	1.5 sccm
	(94 μg/s)
Anode Potential	300 V
Anode Current	1.73 A
Inner Coil Current	1.75 A
Outer Coil Current	1.75 A
Keeper Current	0.5 A
Heater Current	3.0 A
Thrust	22.4 mN
Anode Efficiency	31%
Specific Impulse	1440 s

also influence the fluorescence lineshape[10] and must be accounted for when analyzing the lineshapes should the fields be of sufficient magnitude. In the case of LIF of ions in a Hall effect thruster, the fluorescence lineshape appears to be most indicative of the aforementioned plasma turbulence including periodicity in the positions of the ionization zone within the acceleration channel.

AFRL has examined the spectroscopy of the krypton ions and has developed LIF capabilities with regard to the 728.98 nm $5d^4D_{7/2}$–$5p^4P^{\circ}_{5/2}$ Kr II transition.[11, 12] The details of applicaiton of LIF using the metastable $5d^4D_{7/2}$ state and exciting to the $5p^4P^{\circ}_{5/2}$ state using a laser at 728.98 nm are detailed in those papers.

Apparatus

Vacuum Facility and Thruster

The LIF measurements were performed in Chamber 6 of the Air Force Research Laboratory (AFRL) Electric Propulsion Laboratory at Edwards AFB, CA. Chamber 6 is a non-magnetic stainless steel chamber with a 1.8 m diameter and 3 m length. Pumping is provided by four single stage cryogenic panels (single stage cold heads at 25 K) and one 50 cm two stage cryogenic pump (12 K). This vacuum test chamber has a measured maximum pumping speed of 36,000 L/s on xenon and krypton.

The Hall thruster used in this study is a medium power laboratory Hall effect thruster which has been described elsewhere.[13] This thruster is designed for operation on xenon and performance is not well characterized for krypton, although extensive plume measurements are available.[14] Thruster operation for this effort consisted of a single stable condition shown on Table 2. Unpublished thrust measurements from our laboratory show krypton operation of the BHT-600 at the conditions in Table 2 yields a thrust of 22.4 mN corresponding to an anode efficiency of approximately 31%.

Chamber pressure during thruster operation was measured with a cold cathode ionization gauge and is approximately 3×10^{-3} Pa, corrected for krypton (using an N_2 conversion to Kr multiplicative factor of 0.59[15]). During thruster operation, the thruster parameters shown in Table 2 are monitored and recorded at a 0.2 Hz data rate.

Laser and Optics

The laser used in this study is a custom built ±50 GHz tunable diode laser (Newport Optics, New Focus Division) centered on the $5d^4D_{7/2}$–$5p^4P^{\circ}_{5/2}$ transition with a maximum of 25 mW output power. This laser is a Littman–Metcalf external cavity tunable diode laser capable of mode hop free tuning across approximately 100 GHz tuning range at output powers as high as 25 mW with a line width of less than 500 kHz.

Based on previous efforts,[16] the laser, probe beam launch optics, and fluorescence collection optics are located on two optical tables placed about viewports with optical access into the vacuum chamber as shown in Fig. 1. On the primary optics table, the diode laser beam first passes through a Faraday isolator to eliminate laser feedback. The laser beam then passes through a 10% wedged beam pick–off (PO) to provide beam diagnostics. The first of the two reflections (each approximately 5% of incident power) is directed onto a photodiode detector (D1) and provides constant power feedback to the laser. The second pick–off beam passes through a 300 MHz free spectral range, high finesse Fabry–Perot etalon (F–P) that provides frequency monitoring of the wavelength interval swept during a laser scan.

The main laser beam is then chopped at 3 kHz by a mechanical optical chopper for phase sensitive detection. It is then divided into two equal components by a 50:50 cube beam splitter (BS). The first component passes through a krypton opto-galvanic cell and is terminated by a beam dump. The opto-galvanic cell current is capacitively coupled to a lock-in amplifier in order to monitor the Kr II 728.98 nm $5d^4D_{7/2}$–$5p^4P^{\circ}_{5/2}$ transition to provide a zero velocity reference.[17]

The probe beam is then directed via several mirrors and focused by a single lens to a sub-millimeter beam waist within the chamber vacuum through a glass vacuum viewport. The fluorescence collection optics also shown in Fig. 1 collect the signal generated at the beam waist. The fluorescence is collected by a 75 mm diameter, 300 mm focal length lens within the chamber. The collimated signal is directed through a window in the chamber side wall to a similar lens that focuses the collected fluorescence onto the entrance slit of 125 mm focal length monochrometer with a photomultiplier tube (PMT) detector. The PMT signal is then analyzed using a second lock-in amplifier. The spatial resolution of the measurements is determined by the geometry of the spectrometer entrance slit (note the 1:1 magnification of the collection optics).
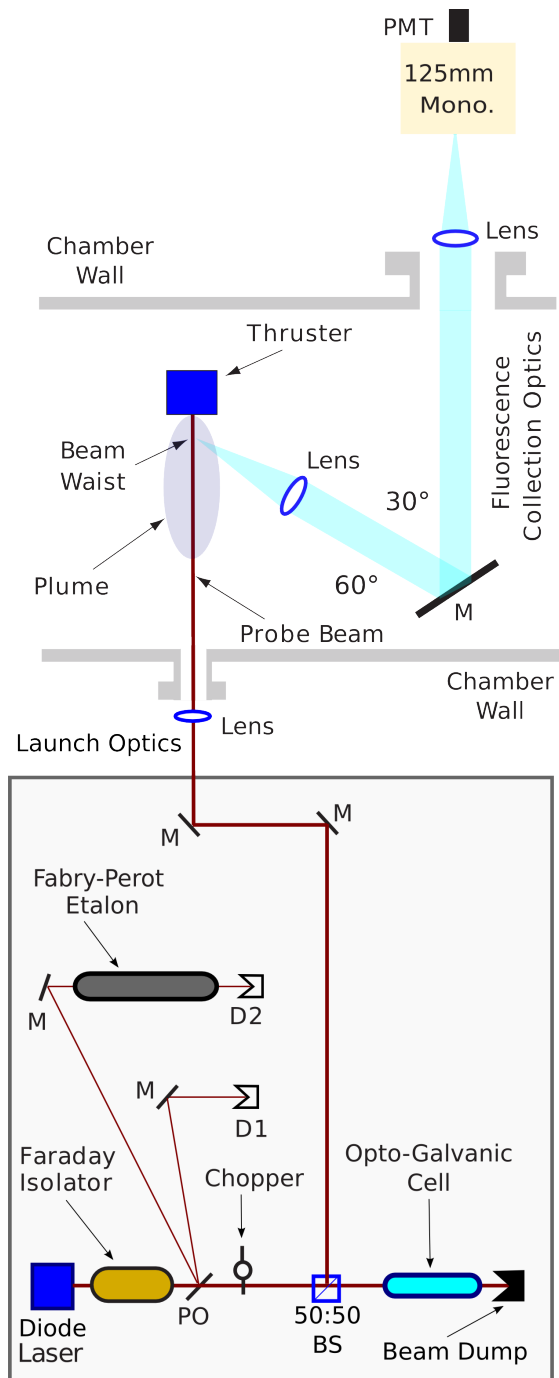
3

Fig. 1   Layout of Kr II laser-induced fluorescence apparatus showing all relevant optical components, portions of the vacuum chamber, and Hall effect thruster thruster plume.

Krypton Velocity Measurements

Measurement Domain

Figure 2 shows a cross-section of the BHT-600 Hall effect thruster used in this test. Annotated in red is the measurement volume. The volume consists of a linear set of data points spaced by 2 mm at X=0, Y=28 mm with Z varying between -8 mm and +12 mm. This measurement set overlaps the measurements of Nakles
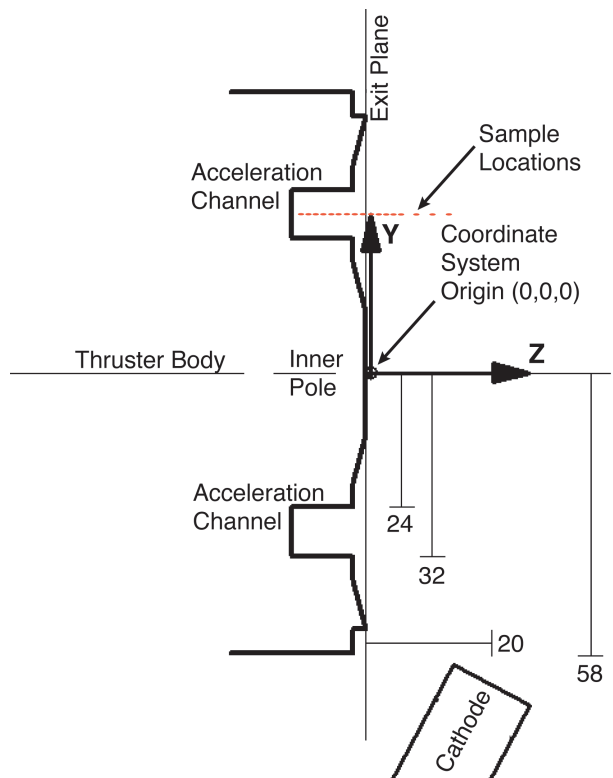

Fig. 2   Cutaway view of the BHT-600 Hall effect thruster with measurement volume shown in red.

and Hargus who measured the xenon acceleration in the same region of the same thruster at similar conditions.[13]

Velocity Distributions

As was stated earlier, the raw fluorescence traces are a reasonable representation of the Kr ion velocity distribution (VDF). Recall that the fluorescence traces measured are the convolution of the true VDF, the transition line shape, and the laser line width. The transition lineshape has been modeled and found to be relatively narrow compared to the fluorescence trace.[11,12] In turn, the laser line width is only approximately 500 kHz. As a result, the fluorescence line shape magnitude is essentially within 10–15% of the time averaged VDF. This is consistent with previous velocity distribution measurements for xenon which showed that deconvolution of the transition lineshape was not necessary in the near plume.[18]

Figure 3 shows the evolution of the velocity distributions of the ionized krypton. Nearest the anode, the VDF at Z = -8 mm shows a slight negative velocity. This is either indicative of the small uncertainties in the measurements, or may alternatively be a manifestation of the ion drag toward the anode by the electron current. These negative velocities are consistent with other previous measurements of xenon Hall effect thrusters.[4,8,9,13]
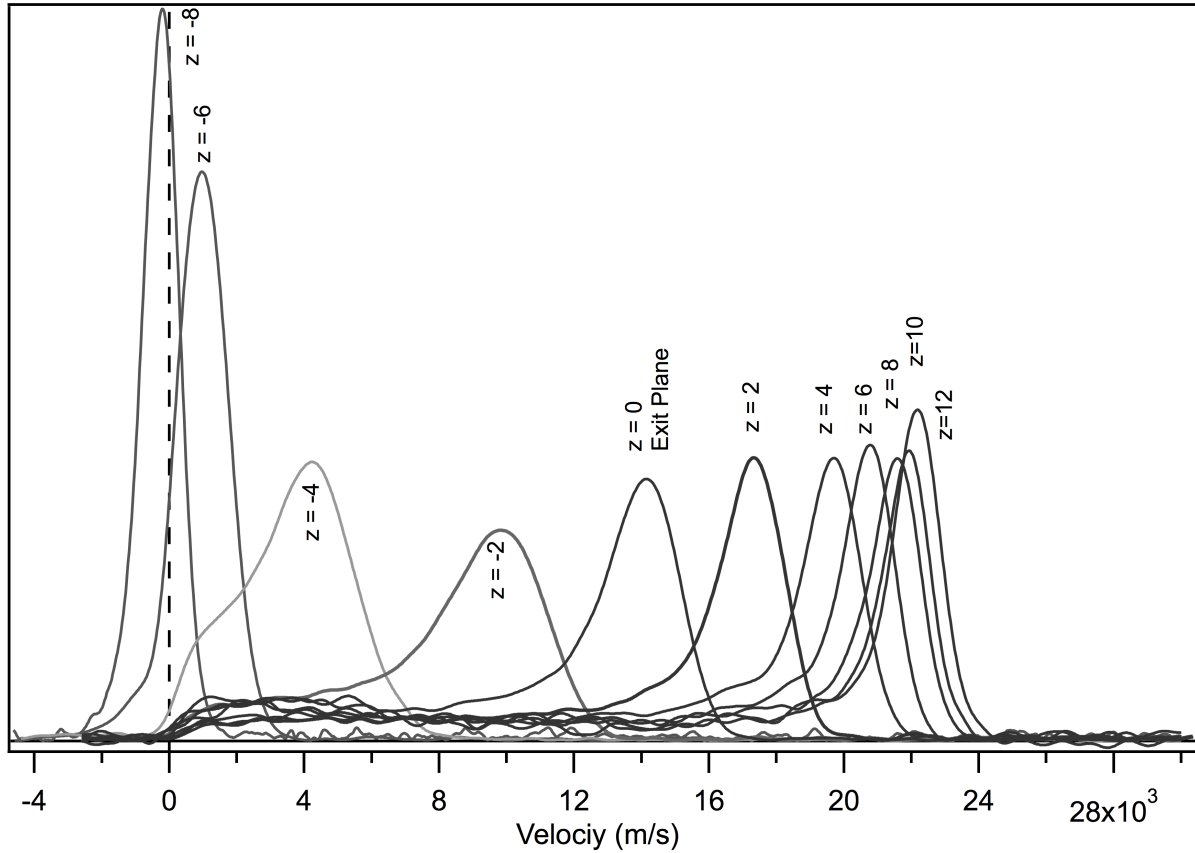
Prior Z = -4 mm, we interpret the krypton ion ve-

Fig. 3 Velocity distributions of krypton ions showing acceleration of the propellant stream from Z = -8 mm to Z = +12 mm. Note that each distribution is individually normalized to unity area.

locity distributions as indicative of a single velocity population; all of whom were created at approximately the same plasma potential and that this region is dominated by ionization with little acceleration. By Z = -4 mm we see that a portion of the velocity distribution has been accelerated to a velocity around 4 km/s, and as high as 8 km/s. However, there is evidence of significant ionization yet occurring as 20–30% of the population has velocities of less than 3 km. Interestingly, we see significant low velocity populations from this axial position onward for all subsequent measurements showing low velocity ion population components. This implies that significant ionization is occurring at all measurement locations, including those in the plume.

Velocity Measurements

Figure 4 shows the most probable velocities measured in the discharge of the BHT-600 Hall effect thruster. The most probable velocities correspond to the peak of the extracted fluorescence curves and are valuable since they provide a singular value that characterizes the behavior of the peak of the velocity distribution. It should be noted that this value is easily extracted with minimum ambiguity from noisy data. It obviously differs from the mean and median velocity values; however, we feel that use of this value provides

an excellent point of comparison so long as the distribution is not particularly broad and the fluorescence has adequate signal to noise ratios (SNR).

The velocity profile in Fig. 4 shows the velocity near zero at Z = -8 mm nearest the anode (at approximately -9 mm). The most probable velocity climbs smoothly, showing maximum acceleration just inside the exit plane (Z=0), to a value just below 24 km/s at Z = +12 mm. It is interesting to note that the velocity at Z = +12 mm does not appear to have peaked and is still rising.

Kinetic Energy and Effective Electric Field

One effective way to illustrate the deposition of energy into the propellant from the discharge is to calculate the profile of propellant kinetic energy. We chose to make this calculation using the most probable velocities shown in Fig. 4. Calculating the kinetic energies of the propellant using $\frac{1}{2}mv^2$ and expressing the units in eV, we arrive at Fig. 5.

In Fig. 5, we see that the energy deposition into the propellant does not begin until approximately Z = -4 mm. The calculated kinetic energies also more clearly show that there is considerable energy deposition occurring between Z = +10 and +12 mm. This indicates that the acceleration extends into the plume,

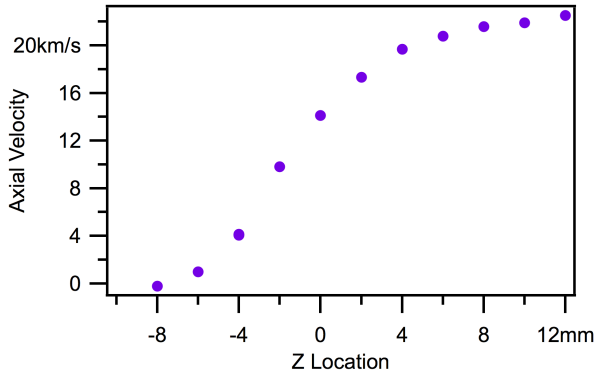**Fig. 4   Most probable krypton velocities of the BHT-600 Hall effect thruster. Note that Z=0 denotes the location of the exit plane**

Fig. 6   Effective electric field acting on krypton propellant. Note that Z=0 denotes the location of the exit plane.
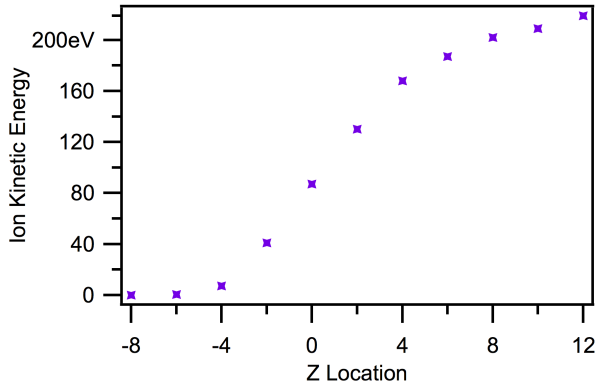

Fig. 5   Propellant kinetic energies calculated from most probable krypton velocities of the BHT-600 Hall effect thruster. Note that Z=0 denotes the location of the exit plane.

Table 3   *Xenon thruster operating conditions.*

Xe Anode Flow	25.5 sccm (2.5 mg/s)
Xe Cathode Flow	1.5 sccm (147 μg/s)
Anode Potential	300 V
Anode Current	1.93 A
Inner Coil Current	1.75 A
Outer Coil Current	1.75 A
Keeper Current	0.5 A
Heater Current	3.0 A
Thrust	35.8 mN
Anode Efficiency	44%
Specific Impulse	1460 s

and likely further than the spatial extent of the measurements. The peak ion energy is approximately 220 eV. This is lower than the 300 V applied discharge potential.

An electric field **E** can be calculated from the derivative of the kinetic energies using the relationship $E_z = -\bigtriangledown_z \phi$. This *effective* electric field is calculated by taking the kinetic energies in Fig. 5, fitting a smoothing spline which is subsequently numerically differentiated. The resultant electric field is believed to be a measure of the *effective* electric field acting on the ions. The use of the most probable velocity at the root of this calculation provides the least ambiguity and greatest repeatability, but most likely is not a true representation of the electric field which has considerable more complexity in both the spatial and temporal domains. With that caution, the effective electric field calculated here is a the only such non-intrusive measurement available.

Figure 6 shows the calculated electric field within the thruster and extending into the near plume. The electric field peaks at 23 kV/m just inside the thruster
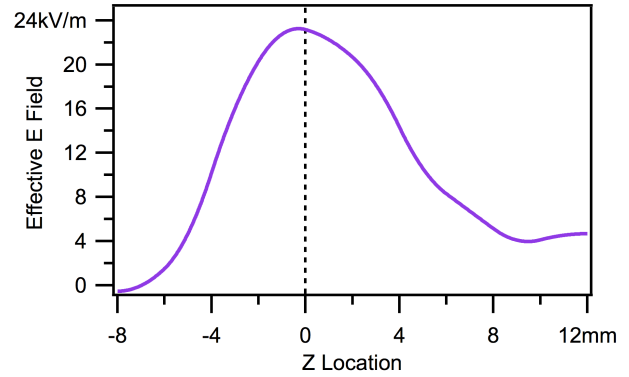
exit plane at Z=0. A significant portion of the electric field is outside the thruster. The magnitude of the electric field is approximately 4 kV/m at Z = +12 which may be an edge effect or an artifact of the small number of measurements.

Comparison to Xenon Acceleration

Nakles and Hargus published results of xenon ion acceleration for the same BHT-600 Hall effect thruster in the region spanning X=0, Y = 28 mm, and Z varying between -9 mm to +10 mm with 1 mm data point spacing within the thruster (Z < 0) and either 1 or 2 mm measurement spacing in the near plume (Z > 0).[13] The thruster operating performance parameters are shown in Table 3

Comparing the values of Tables 2 and 3 is informative. First, due to the higher atomic mass of xenon (131.3 vs 83.8 amu), the delivered thrust is significantly higher for xenon (35.8 vs 22.4 mN). But as noted earlier, it is important to note that the volumetric flow rates (atom flux, or atoms/second) are equal for both xenon and krypton cases discussed here. Interestingly, thruster efficiency is significantly lower for the krypton case than for xenon, and the specific im-

pulse values are approximately the same. Based on atomic mass alone, and assuming equivalent ionization, one would expect the specific impulse of krypton to be 125% that of xenon. The combination of lower energy conversion efficiency and equivalent specific impulse point toward a lower propellant utilization fraction for krypton.

Energy Deposition

Figure 7 compares the energy deposition of the xenon and krypton propellants. The general behavior is very similar, but the krypton energy deposition is consistently lower than that of xenon. Although the acceleration begins in the same region, the rate of acceleration is lower for krypton. This is confirmed by Fig. 8 which presents the effective electric fields for both xenon and krypton.

In Fig. 8, we see that the krypton effective electric field peaks at a substantially lower magnitude and further downstream, closer to the exit plane than it does for xenon. The effective electric fields are not similar in shape as that of krypton is substantially wider. The explanation for this contains two threads. First, as the drift velocity of the neutrals is inversely proportional with atomic mass, the krypton neutrals are likely to travel further out of the thruster channel than the xenon neutrals prior to ionization. As a result, the krypton neutrals have a higher probability of exiting the channel and being lost to electrostatic acceleration. This is reinforced by the krypton effective electric field's larger magnitude outside the thruster in Fig. 8 and by the clear evidence of ionization occurring throughout the measurement region in Fig. 3. Second, the lower oscillatory behavior of krypton may promote lower electric fields simply due to the lessening of turbulent transport. As a result, the electric potential fall will be a larger spatial extent for krypton. The relative importance of these two mechanisms is not yet fully understood, but they both imply a longer channel would be beneficial for a dedicated krypton Hall effect thruster.

Velocity Distributions

Figure 9 presents the velocity distributions measured by Nakles and Hargus.[13] Compared to Fig. 3, the xenon velocity distributions in Fig. 9 have substantial differences. First of all, the xenon velocity distributions are much broader. This appears to be a function of the oscillatory behavior of the anode discharge and is quantified by Nakles and Hargus, as due to thruster *breathing mode* where an axial ionization wave first forms near the anode and then travels out into the plume. In the plume the ionization wave dissipates whereupon it reforms at the anode once more, usually with frequencies of a few to several tens of kHz.

At the conditions examined in this work, xenon exhibits a strong breathing mode anode current oscillation which dominates the anode current. On the
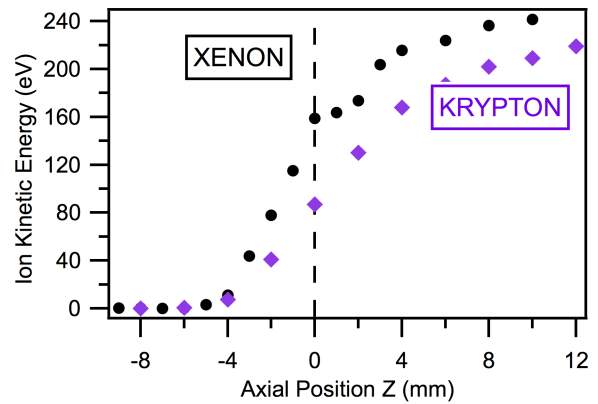

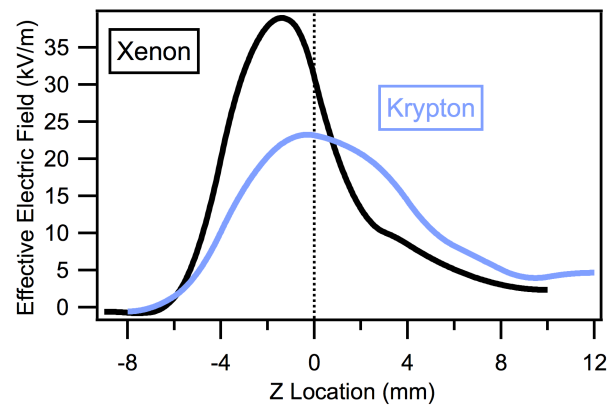**Fig. 7   Comparison of krypton and ion kinetic energies.**

Fig. 8   Comparison of krypton and ion kinetic energies.

other hand, krypton is very much quiescent and the breathing mode here manifests itself as a small current ripple on the generally DC anode current. It is believed that the breathing mode oscillations enhance electron transport since although the ionization wave ultimately travels outward in the axial direction, it is also composed of a series of azimuthal instabilities which promote cross-field electron transport also known as Bohm diffusion, or the so called *anomalous diffusion*.[19] As a result, the xenon velocity distributions are much broader as the electron cross–field transport enhancing strong ionization wave traverses the acceleration channel and dissipates somewhere in the near plume, all the while temporally broadening the electric field. Evidence of this is shown in Fig. 9 starting at Z = -4 mm where we have evidence of ionization (zero velocity ions) and a high velocity tail extending approximately 12 km/s, much higher than the most probable velocity of 4 km/s. There is no equivalent behavior in the krypton velocity distributions of Fig. 3.

Another difference is the significant proportion of low velocity krypton ions and evidence of ionization
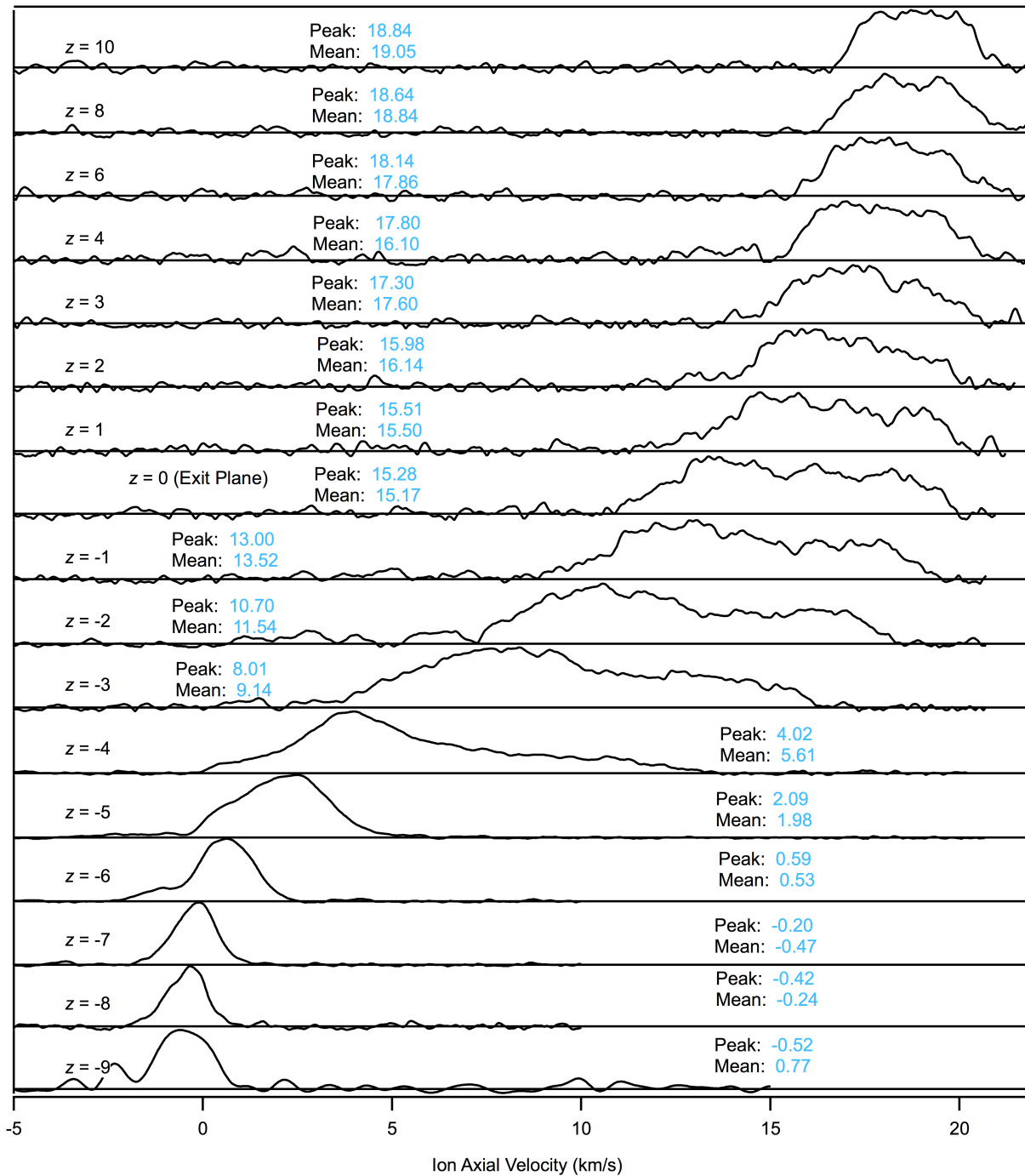
Fig. 9 Xenon velocity distributions taken from Nakles and Hargus[13] Peak (most probable) and mean (population weighted) velocities are given for each velocity distribution in km/s.

occurring through out the acceleration channel and into the plume. For example, at Z = +12 mm, the velocity distribution in Fig. 3 is 35–40% in the low velocity region (defined as below 18 km/s, where the most probable velocity is 22.4 km/s and the resulting mean velocity of the distribution is 16.8 km/s. It bears consideration that while 35–40% of the ions are in the low velocity region, this region only contains 15% of the velocity distribution's energy.

The efficiency in energy conversion for krypton is substantially lower than that of xenon. The lower specific impulse for krypton is a symptom of this inefficiency. The energy deposition and electric field plots in Figs. 8 and 7 show that for this particular case, krypton is not able to match the energy deposition of xenon. Comparison of Figs. 9 and 3 show that krypton is ionizing substantial propellant far downstream of the acceleration potential. As a result, much of the krypton propellant that is ionized can not fully utilize the applied acceleration potential, and another significant neutral fraction leaves the thruster as neutrals completely oblivious to the applied potential.

Conclusions and Future Work

Comparison of xenon and krypton for a single thruster operating parameter where the atomic flow rate, applied potential, and applied radial magnetic field are all equal demonstrated that changes in propellant result in dramatic changes in the acceleration of the propellant both within and in the near plume of a medium power Hall effect thruster. We have chosen to examine a near nominal xenon case with a krypton case with the same applied parameters. As a result the Hall effect thruster designed and optimized for xenon performed significantly worse for krypton. The LIF diagnostic allowed us to identify energy deposition and propellant utilization as the primary culprits for this particular set of operating parameters.

It is evident that examination of single flow rate is a not fully adequate comparison of these two thrusters. For example, the most probable ion velocities are about 15% higher for krypton with a resultant lower plasma density. Electron cross-field transport is almost certainly affected by the significantly lower breathing mode of krypton. Also consider that the ionization potential of krypton is 16% higher than that of xenon and krypton has a lower electron collision ionization cross-section. These facts imply that a better krypton performance condition exists. Past performance measurements have shown that a higher performance for krypton is possible with higher flows and higher acceleration potential. The net effect appears of this change would be to increase the plasma density at the location of ionization and produce a higher plasma density gradient in the accelerated ion stream. Future work will examine an optimized krypton operating condition to compare its acceleration to

the cases presented in this work.

One further issue may require attention at some point in the future should krypton Hall effect thruster development efforts continue. Significant resources have been expended to develop design rules for xenon fueled Hall effect thrusters. There appears to be considerable uncertainty how these design rules may change with propellant. For example, performance issues with krypton in Hall effect thrusters designed for xenon have oftentimes been dismissed as due to design optimization for xenon. We are not aware of any experimental optimization of krypton performance. Usually, krypton performance measurements are performed on a Hall effect thruster as a addendum to xenon testing, or as a cost saving strategy. As a result, these studies, and others like it, have value since they provide fundamental data; however, application of these sorts of advanced diagnostics will also provide fundamental insights as to the operation of these notoriously complex plasma discharges.

References

[1] R. Jahn, *Physics of Electric Propulsion*. McGraw-Hill, 1968.

[2] D. R. Lide, *Handbook of Chemistry and Physics*, 79th ed. CRC Press, 1998.

[3] O. Duchemin, D. Valentian, and N. Cornu, "Cryostorage of propellants for electric propulsion," in *Proceedings of the 45th Joint Propulsion Conference and Exhibit*, no. AIAA-2009-4912. American Institute of Aeronautics and Astronautics, August 2009.

[4] W. A. Hargus Jr. and M. A. Cappelli, "Laser-induced fluorescence measurements of velocity within a hall discharge," *Applied Physics B*, vol. 72, no. 8, pp. 961–969, June 2001.

[5] W. A. Hargus and C. S. Charles, "Near exit plane velocity field of a 200 w hall thruster," *Journal of Propulsion and Power*, vol. 24, no. 1, pp. 127–133, January-February 2008.

[6] S. Mazouffre, D. Gawron, V. Kulaev, and N. Sadeghi, "A laser spectroscopic study on xe+ ion transport phenomena in a 5 kw-class hall effect thruster," in *Proceedings of the 30th International Electric Propulsion Conference*, no. IEPC-2007-160. Florence, Italy: Electric Rocket Society, September 2007.

[7] W. Demtroder, *Laser Spectroscopy: Basic Concepts and Instrumentation*. Springer-Verlag, 1996.

[8] M. R. Nakles and W. A. Hargus Jr., "Background pressure effects on internal and near-field ion velocity distribution of the bht-600 hall thruster," in *Proceedings of the 44th Joint Propulsion Conference and Exhibit*, no. AIAA-2008-5101. Hartford, CT: American Institute of Aeronautics and Astronautics, July 2008.

[9] W. A. Hargus Jr., M. R. Nakles, B. Pote, and R. Tedrake, "The effect of thruster oscillations on axial velocity distributions," in *Proceedings of the 44th Joint Propulsion Conference and Exhibit*, no. AIAA-2008-4724. Hartford, CT: American Institute of Aeronautics and Astronautics, July 2008.

[10] T. Fujimoto and A. Iwamae, Eds., *Plasma Polarization Spectroscopy*, ser. Series on Atomic, Optical and Plasma Physics.   Springer-Verlag, 2008, vol. 44.

[11] W. A. Hargus, "A preliminary study of krypton laser-induced fluorescence," in *Proceedings of the 46th Joint Propulsion Conference and Exhibit*, no. AIAA-2010-6524.   American Institute of Aeronautics and Astronautics, August 2010.

[12] W. A. Hargus, G. M. Azarnia, and M. R. Nakles, "Demonstration of laser-induced fluorescence on a krypton hall effect thruster," in *Proceedings of the 32nd International Electric Propulsion Conference*, no. IEPC-2011-018.   Electric Rocket Society, September 2011.

[13] M. R. Nakles and W. A. Hargus, "Background pressure effects on ion velocity distribution within a medium-power hall thruster," *AIAA Journal of Propulsion and Power*, vol. 27, no. 4, pp. 737–743, July-August 2011.

[14] M. R. Nakles, R. R. Barry, C. W. Larson, and W. A. Hargus, "A plume comparison of xenon and krypton propellant on a 600 w hall thruster," in *Proceedings of the 31st International Electric Propulsion Conference*, no. IEPC-2009-118, Ann Arbor, MI, September 2009.

[15] I. Leybold-Heraeus Vacuum Proucts, *Vacuum Technology its Foundations Formulae and Tables*.   Leybold-Heraeus Vacuum Proucts, Inc., 1987.

[16] W. A. Hargus and M. R. Nakles, "Ion velocity measurements within the acceleration channel of low-power hall thruster," *IEEE Transactions on Plasma Science*, vol. 36, no. 5, pp. 1989–1997, October 2008.

[17] B. Barbieri, N. Beverini, and A. Sasso, "Optogalvanic spectroscopy," *Review of Modern Physics*, vol. 62, no. 3, pp. 603–644, July 1990.

[18] W. A. Hargus Jr. and M. R. Nakles, "Evolution of the ion velocity distribution in the near field of the bht-200-x3 hall thruster," in *Proceedings of the 42nd Joint Propulsion Conference and Exhibit*, no. AIAA-2006-4991.   Sacramento, CA: American Institute of Aeronautics and Astronautics, July 2006.

[19] S. Yoshikawa and D. J. Rose, "Anomalous diffusion of a plasma across a magnetic field," *Physics of Fluids*, vol. 5, no. 3, March 1963.